

CoPt/Ag nanocomposites with (001) texture

V. Karanasos, I. Panagiotopoulos, D. Niarchos, H. Okumura, and G. C. Hadjipanayis

Citation: *Appl. Phys. Lett.* **79**, 1255 (2001); doi: 10.1063/1.1397762

View online: <http://dx.doi.org/10.1063/1.1397762>

View Table of Contents: <http://apl.aip.org/resource/1/APPLAB/v79/i9>

Published by the [American Institute of Physics](#).

Related Articles

Transmittance and optical constants of Sr films in the 6–1220eV spectral range

J. Appl. Phys. **111**, 113533 (2012)

Kinetic behavior of nitrogen penetration into indium double layer improving the smoothness of InN film

J. Appl. Phys. **111**, 113528 (2012)

Detection of filament formation in forming-free resistive switching SrTiO₃ devices with Ti top electrodes

Appl. Phys. Lett. **100**, 223503 (2012)

Direct measurement of lateral macrostep velocity on an AlN vicinal surface by transmission electron microscopy

J. Appl. Phys. **111**, 103529 (2012)

Structural modifications of zinc phthalocyanine thin films for organic photovoltaic applications

J. Appl. Phys. **111**, 103117 (2012)

Additional information on *Appl. Phys. Lett.*

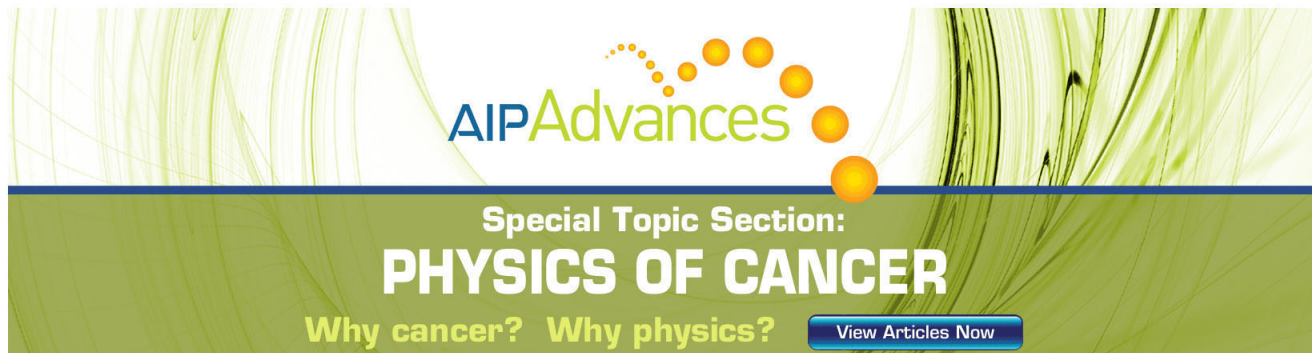
Journal Homepage: <http://apl.aip.org/>

Journal Information: http://apl.aip.org/about/about_the_journal

Top downloads: http://apl.aip.org/features/most_downloaded

Information for Authors: <http://apl.aip.org/authors>

ADVERTISEMENT

The advertisement features a green and white background with a pattern of thin, vertical lines. At the top, the 'AIP Advances' logo is displayed, with 'AIP' in blue and 'Advances' in green. Below the logo, the text 'Special Topic Section: PHYSICS OF CANCER' is written in white. Underneath, the phrase 'Why cancer? Why physics?' is written in green. A blue button with white text 'View Articles Now' is located at the bottom right of the advertisement.

CoPt/Ag nanocomposites with (001) texture

V. Karanasos,^{a)} I. Panagiotopoulos, and D. Niarchos
 IMS, NCSR "Demokritos," Ag. Paraskevi Attiki, 153 10 Greece

H. Okumura and G. C. Hadjipanayis
 Department of Physics and Astronomy, University of Delaware, Newark, Delaware 19716

(Received 4 May 2001; accepted for publication 6 July 2001)

CoPt/Ag nanocomposites with the tetragonal ($L1_0$) structure have been prepared by magnetron sputtering. The dependence of texture on film thickness, bilayer thickness, CoPt volume fraction, and annealing conditions is investigated. Films with a thickness below 15 nm consist of islands with (001) texture while as the thickness increases, the islands coalesce into a continuous film and the (111) texture appears. Microstrain is minimized in the range of film thickness where the (001) texturing is optimum indicating that strain energy provides the driving force of (001) growth texturing. The (001) texture improves with CoPt volume fraction for all annealing times but disappears above 95 vol% indicating that the existence of the Ag plays an important role in the development of the (001) texture. © 2001 American Institute of Physics.
 [DOI: 10.1063/1.1397762]

Sputter deposited nanocomposites consisting of CoPt (or FePt) particles, with the high magnetic anisotropy $L1_0$ structure have attracted attention due to their possible use as ultrahigh density recording media.¹⁻⁸ A disadvantage of the sputter deposited nanocomposites is their tendency to grow with a (111) texture thus having the easy-magnetization direction (001) at an angle of 36° above the film plane. Recently, a (001) texture has been found in CoPt/SiO₂ granular films with small Ag additions⁹ as well as in FePt/B₂O₃ nanocomposites.¹⁰ The reason for this c -axis orientation is not clear yet. In this study, we examine the evolution of texture and microstructure of CoPt/Ag granular films with film thickness, bilayer thickness, CoPt volume fraction, and annealing conditions, in order to elucidate the mechanism of texturing in these materials.

The CoPt/Ag films were deposited by magnetron sputtering. Preparation details have been published elsewhere.^{1,4,8} The CoPt and Ag layers are successively deposited in a multilayer form starting by the Ag layer deposition. X-ray diffraction (XRD) spectra were collected with a SIEMENS D500 powder diffractometer using Cu $K\alpha$ radiation. Magnetization measurements were performed with a Quantum Design superconducting quantum interference device magnetometer. The as-deposited films are magnetically soft and their XRD patterns indicate a multilayered structure with (111) texture. In order to crystallize the high anisotropy $L1_0$ phase, the films were annealed *in situ* at a pressure of 10^{-6} Torr at 600 °C for 20, 40, and 70 min. The microstructure was examined with a Digital Instruments NanoScope III atomic force microscope (AFM) and a Jeol JEM 2000 FX transmission electron microscope (TEM).

In the following, for brevity, we denote the samples in the form $(t_{\text{CoPt}}/t_{\text{Ag}})_N$ where t_{Ag} and t_{CoPt} are the thickness of the Ag and CoPt layers, respectively (in nm), and N is the number of repetitions of the bilayer.

The (00 ℓ) reflections dominate the XRD pattern of

films with $\delta < 15$ nm indicating a high degree of preferential orientation of the c -axis perpendicular to the film plane. The hysteresis loops of the (3/1)₃ film (annealed at 600 °C for 20 min) in Fig. 1 show a clear perpendicular anisotropy with $H_C = 4.2$ kOe and squareness $S = 0.88$ when measured with the applied field perpendicular to the film plane whereas when the applied field is parallel to the film plane $H_C = 1$ kOe and $S = 0.12$. The (001) peak rocking curve of this sample (shown in the inset of Fig. 1) has a full width at half maximum of 5° confirming the high degree of texturing. For thicker films with the (111) texture, the loops measured with the applied field parallel and perpendicular to the substrate do not differ substantially.

Three different series of film samples were prepared in order to study the effect of the bilayer thickness $\Lambda = t_{\text{CoPt}} + t_{\text{Ag}}$ as well as the effects of the nominal film thickness $\delta = N\Lambda$ and of the CoPt volume fraction. The first series was of the form $(3/4\Lambda/1/4\Lambda)_3$ with Λ ranging from 2 to 10 nm resulting in a total thickness δ between 6 and 30 nm while the second was of the form $(3/1)_N$ with N between 1 and 5 resulting in δ between 4 and 20 nm and a fixed bilayer thick-

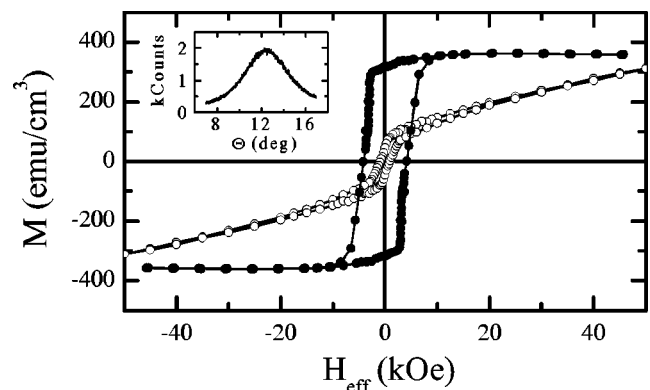


FIG. 1. Hysteresis loops measured parallel (open circles) and perpendicular (closed circles) to the film plane for a film with (001) texture and thickness $\delta = 12$ nm are shown. The inset shows the rocking curve of the (001) peak.

^{a)}Electronic mail: bkaranasos@ims.demokritos.gr

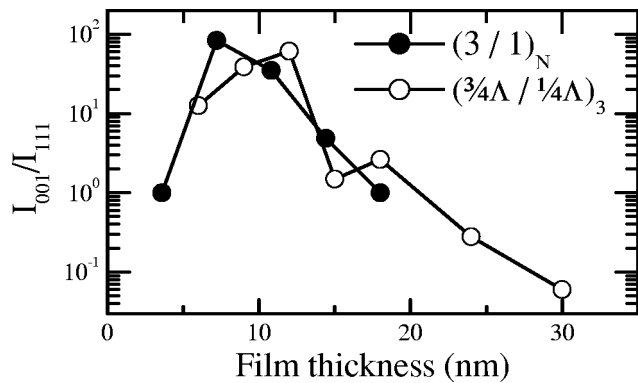


FIG. 2. The ratio of the (001) peak intensity to that of the (111) peak (I_{001}/I_{111}) as a function of δ for two series of samples $(3/1)_N$ (solid circles) and $(\frac{3}{4}\Lambda/\frac{1}{4}\Lambda)_3$ (open circles).

ness $\Lambda=4$ nm. Both series correspond to a CoPt volume fraction of 75%. The ratio of the (001) peak intensity to that of the (111) peak (I_{001}/I_{111}) is used as a figure-of-merit of the degree of (001) texturing and it is plotted as a function of δ for both series in Fig. 2. The degree of (001) texturing is drastically increased with decreasing δ , goes through a maximum around 10 nm, and slowly decreases at lower δ . The coincidence of the two curves indicates that the degree of texturing is mainly determined by the total thickness rather than by the bilayer thickness. The competition between anisotropic surface energy¹¹ and elastic energy terms^{12–14} is known to drive the preferential growth of grains with specific crystallographic orientations in thin films. Thickness dependence of texture may arise from the fact that the latter is thickness dependent unlike the former. Strain energy, in turn, is influenced by the specifics of film growth as island formation and coalescence¹⁵ or changes in grain morphology.¹³

In order to study the reasons of the thickness dependence of the texturing, the microstructure was monitored as a function of thickness. Selected TEM pictures showing the evolution of microstructure as a function of δ are presented in Fig. 3. The $(1.5/0.5)_3$ sample (nominal $\delta=6$ nm) consists of isolated particles covering only 20% of the total substrate area. The $(3/1)_3$ sample (nominal $\delta=12$ nm) is close to the percolation limit of those particles which cover the 40% of the total substrate area whereas for the $(7.5/2.5)_3$, the full substrate area is covered. These observations have been also confirmed by AFM data. Cross sectional TEM studies (Fig. 4) verify that the $(3/1)_3$ sample (nominal $\delta=12$ nm) consists of isolated CoPt islands with a thickness of 30 nm and a large in-plane diameter. The increased (with respect to the nominal one δ) island thickness is consistent with the fact that the substrate is partially covered. In most of the cases, the islands consist of more than three grains with a size equal to the island thickness.

Microstrain and grain size were estimated by multiple line analysis of the (001), (002), and (003) XRD peaks with the WINFIT1.2 program¹⁶ based on the Fourier method of Warren–Averbach.¹⁷ The results were also verified by Williamson–Hall plots¹⁸ and single line profile analysis.¹⁹ The results are sketched as a function of the nominal film thickness δ in Fig. 5. It can be observed that in the range of film thickness where the (001) texturing is optimum, strain is minimized. The corresponding reduction of mechanical

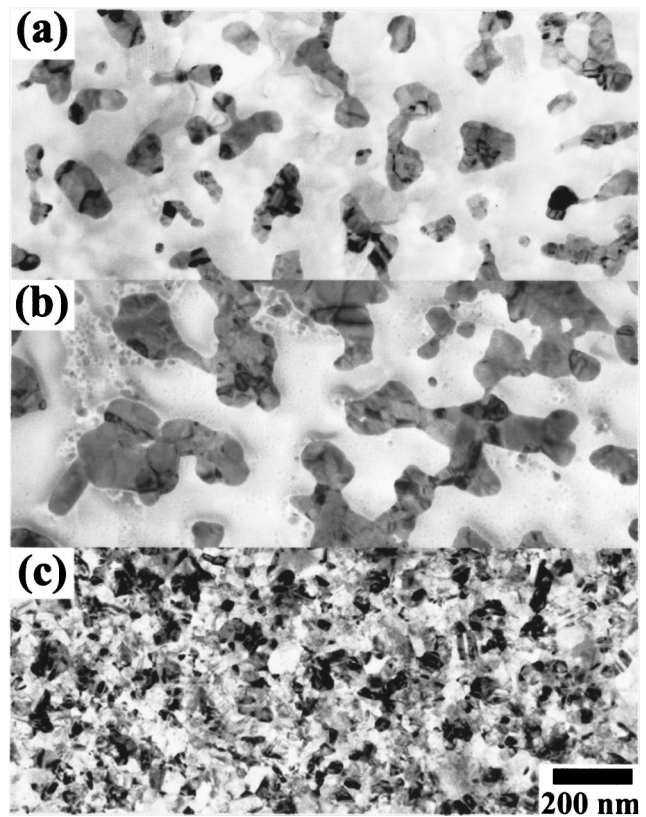


FIG. 3. Planar TEM micrographs of three films with thickness (a) $\delta=6$ nm, (b) $\delta=12$ nm, and (c) $\delta=30$ nm.

strain energy, probably related to the island formation, provides a driving force for the (001) texture. Since in our $\theta-2\theta$ measurements the scattering vector is perpendicular to the substrate, the aforementioned analysis gives the grain dimension D along the film normal. D shows a drastic decrease above 12 nm in accordance with the microscopy studies which indicate the formation of a continuous film above that thickness.

It is worth noting that if the deposition starts with a CoPt layer, the obtained degree of texturing is degraded. This is a further indication that a surface energy term may be important to the development of texture in these films. In order to study the effect of the Ag content, a $(x/4-x)_3$ series with $x=2.5$ to 3.8 nm corresponding to a CoPt volume fraction between 62.5% and 95% (and fixed $\Lambda=4$ nm) has been prepared. This series was subsequently heat treated at 600 °C for 20, 40, and 70 min to monitor the evolution of texturing with

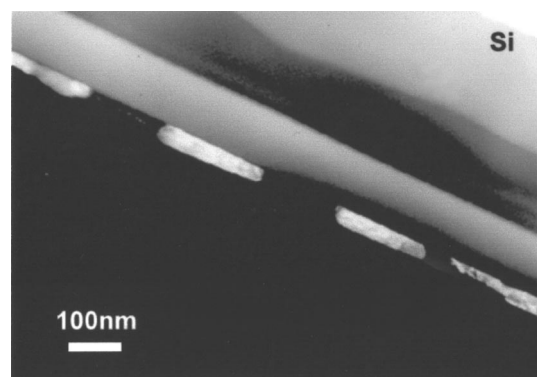


FIG. 4. Cross sectional TEM micrograph of the $(3/1)_3$ sample.

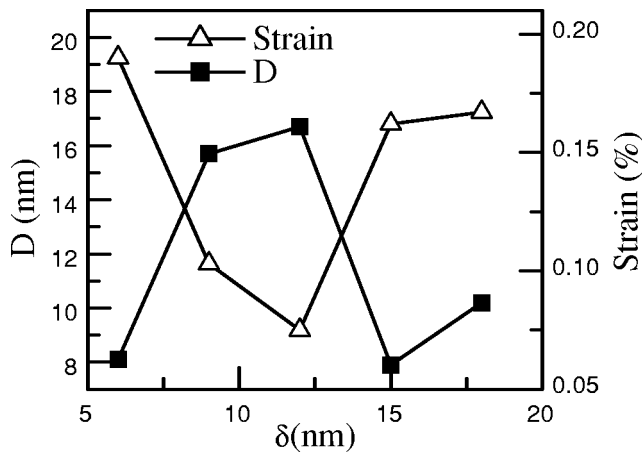


FIG. 5. Microstrain and grain size as a function of the nominal film thickness δ .

annealing time. The I_{001}/I_{111} ratio is plotted against the CoPt volume fraction for the three different annealing times in Fig. 6. The (001) texture initially improves with CoPt volume fraction for all annealing times but disappears above 90

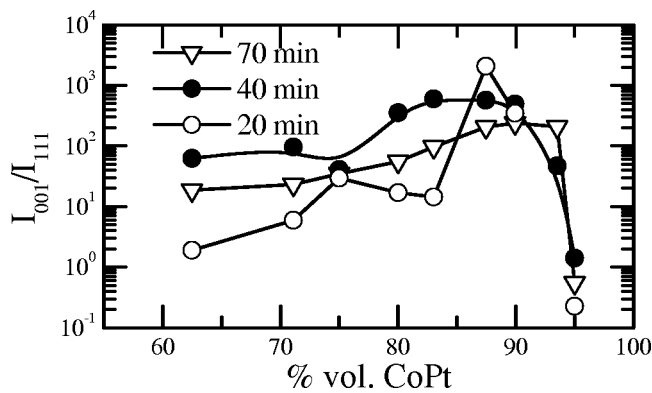


FIG. 6. The I_{001}/I_{111} ratio as a function of CoPt volume fraction for samples annealed at 600 °C for 20, 40, and 70 min.

vol % CoPt. This indicates the existence of the Ag plays an important role in the development of the (001) texture.

In conclusion we have investigated the dependence of texture in CoPt/Ag films on film thickness, bilayer thickness, and annealing conditions. Microscopy and XRD data indicate that at low film thickness, the films are comprised of islands with (001) texture. As the thickness increases, the islands coalesce into a continuous film and the (111) texture appears. The existence of Ag is proven to be essential for the development of texture, even at a volume fraction as small as 10%.

- ¹ S. Stavroyiannis, I. Panagiotopoulos, D. Niarchos, J. A. Christodoulides, Y. Zhang, and G. C. Hadjipanayis, *Appl. Phys. Lett.* **73**, 3453 (1998).
- ² Bo-Bian, K. Sato, Y. Hirotsu, and A. Makino, *Appl. Phys. Lett.* **75**, 3686 (1999).
- ³ M. Yu, Y. Liu, A. Moser, D. Weller, and D. J. Sellmyer, *Appl. Phys. Lett.* **75**, 3992 (1999).
- ⁴ Panagiotopoulos, S. Stavroyiannis, D. Niarchos, J. A. Christodoulides, Y. Zhang, and G. C. Hadjipanayis, *J. Appl. Phys.* **87**, 4358 (2000).
- ⁵ C. Chen, O. Kitakami, S. Okamoto, and Y. Shimada, *J. Appl. Phys.* **87**, 6947 (2000).
- ⁶ A. Kikitsu, A. Murayama, K. Hyomi, and C. M. Falco, *J. Appl. Phys.* **87**, 6944 (2000).
- ⁷ C.-M. Kuo and P. C. Kuo, *J. Appl. Phys.* **87**, 419 (2000).
- ⁸ V. Karanasos, I. Panagiotopoulos, D. Niarchos, H. Okumura, and G. C. Hadjipanayis, *J. Appl. Phys.* **88**, 2740 (2000).
- ⁹ C. Chen, O. Kitakami, S. Okamoto, and Y. Shimada, *Appl. Phys. Lett.* **76**, 3218 (2000).
- ¹⁰ C. P. Luo, S. H. Liou, L. Gao, Y. Liu, and D. J. Sellmyer, *Appl. Phys. Lett.* **77**, 2225 (2000).
- ¹¹ J. P. Perdew, Y. Wang, and E. Engel, *Phys. Rev. E* **66**, 508 (1991).
- ¹² R. Carel, C. V. Thomson, and H. J. Frost, *Acta Mater.* **44**, 2479 (1996).
- ¹³ Y. Zeng, T. L. Alford, Y. L. Zou, A. Amali, B. Manfred Ullrich, F. Deng, and S. S. Lau, *J. Appl. Phys.* **83**, 779 (1998).
- ¹⁴ J. E. Greene, J.-E. Sundgren, L. Hultman, I. Petrov, and D. B. Bergstrom, *Appl. Phys. Lett.* **67**, 2928 (1995).
- ¹⁵ R. Schuster, H. Roder, K. Bromann, H. Brune, and K. Kern, *Phys. Rev. B* **54**, 13476 (1996).
- ¹⁶ S. Krumm, *Mater. Sci. Forum* **228**, 183 (1996).
- ¹⁷ B. E. Warren, *X-Ray Diffraction* (Addison-Wesley, Reading, MA, 1969).
- ¹⁸ G. K. Williamson and W. H. Hall, *Acta Metallica* **1**, 22 (1953).
- ¹⁹ T. H. De Keijser, J. I. Langford, E. J. Mettemeijer, and A. B. P. Vogels, *J. Appl. Crystallogr.* **15**, 308 (1982).